

Privacy-Aware Detection of Fake Identity Documents: Methodology, Benchmark, and Improved Detection Methods (FakeIDet2)

Javier Muñoz-Haro, Ruben Tolosana, Ruben Vera-Rodriguez,
Aythami Morales, Julian Fierrez

*Biometrics and Data Pattern Analytics Lab, Universidad Autónoma de Madrid, Ciudad
Universitaria de Cantoblanco, Madrid, 28049, Madrid, Spain*

Abstract

Remote user verification in Internet-based applications is becoming increasingly important nowadays. A popular scenario for it consists of submitting a picture of the user's Identity Document (ID) to a service platform, authenticating its veracity, and then granting access to the requested digital service. An ID is well-suited to verify the identity of an individual, since it is government issued, unique, and nontransferable. However, with recent advances in Artificial Intelligence (AI), attackers can surpass security measures in IDs and create very realistic physical and synthetic fake IDs. Researchers are now trying to develop methods to detect an ever-growing number of these AI-based fakes that are almost indistinguishable from authentic (*bona fide*) IDs. In this counterattack effort, researchers are faced with an important challenge: the difficulty in using real data to train fake ID detectors. This real data scarcity for research and development is originated by the sensitive nature of these documents, which are usually kept private by the ID owners (the users) and the ID Holders (e.g., government, police, bank, etc.). The present study proposes a new privacy-aware methodology for research and development in fake ID detection that promotes collaboration between ID holders and AI researchers. In practice, the main contributions of our study are: 1) We present and discuss our proposed patch-based methodology to preserve privacy in fake ID detection research. 2) We provide a new public database, FakeIDet2-db, comprising over 900K real/fake ID patches extracted from 2,000 ID images, acquired using different smartphone sensors, illumination and height conditions, etc. In addition, three physical attacks are considered: print, screen, and composite. 3) We present a new privacy-aware fake ID detection method, FakeIDet2, which introduces two novel learnable modules: Patch Embedding Extractor and Patch Embedding Fusion. 4) We release a standard reproducible benchmark that considers physical and synthetic attacks from popular databases in the literature. The results achieved by our proposed FakeIDet2 in detecting very realistic fake IDs under unseen type of attacks are encouraging: 8.90% and 13.84% Equal Error Rate (EER) in the very challenging datasets DLC-2021 and KID34K, respectively. FakeIDet2-db and the accompanying benchmark are publicly available¹.

¹<https://github.com/BiDAIlab/FakeIDet2-db>

1. Introduction

The veracity of digital information is one of the great challenges of society today [2, 37]. With the great advances made in the field of GenerativeAI [24], it is possible to synthesize non-existent content [20], or to modify existing one [28], using simple and fast toolbox available on the internet. These methods can be used for good purposes, e.g., correct biases [29] or improve performance in some scenarios where data scarcity is present [21, 31], but they have their downsides, as they can also be used for malicious purposes such as DeepFakes [34, 35] or misinformation [18]. Evidences of the latter have been found in recent news, where tampered¹ or synthetic² documents were used for underage alcohol purchase or bypass remote verification systems such as Know Your Customer (KYC) to access digital services such as crypto-exchanges or digital banking.

In order to advance in this challenging topic, the present study focuses on Presentation Attack Detection (PAD) [15, 11] on Identity Documents (IDs). Concretely, as can be seen in Fig. 1, we focus on the most popular physical attacks in real-world scenarios: *i) print* attacks are physical fake IDs created using an image or a scanned Identity Document (ID), which is printed on glossy paper to resemble the texture and appearance of real IDs; *ii) screen* attacks, which consist in taking a picture of an ID displayed on a digital screen such as a laptop, tablet, or smartphone; and *iii) composite* attacks, which do not require to tamper an entire document, but only small portions, such as date of birth, family name or the portrait image from the ID owner. In the particular case of *physical composite* attacks, the impostor first prints fields with fake information on colored paper that resembles the colors of the target ID, and crop each field. After that, these crops are lied on the ID document, occluding the original information with the fake one. All these kinds of attacks, a.k.a Presentation Attack Instruments (PAIs), are currently being used by attackers to surpass KYC procedures, which explicitly require capturing live images of the user’s ID using an smartphone camera, granting them access to digital services using fake identities.

Several studies have preliminary analyzed the problem of fake ID detection, proposing very valuable ideas and resources [5, 8, 13]. However, there are several limitations in the field that must still be covered to properly advance in this research direction. First, there are no public databases with official (a.k.a. bona fide) IDs acquired in variable conditions, nor a standard benchmark that evaluates the performance of fake ID detection systems on real-world scenarios. So far, all public databases in the literature consider as “real” IDs those created by researchers in laboratory conditions, not official governments. From now on, we refer to these non-official IDs created by research groups as “real”. As a result, these “real” IDs lack important information and patterns such as watermarks, not representing therefore a fidelity scenario of the problem. Some efforts have been recently carried out in this direction through the organization

¹<https://www.nytimes.com/2025/02/13/nyregion/students-high-tech-fake-ids.html>

²<https://www.404media.co/inside-the-underground-site-where-ai-neural-networks-churn-out-fake-ids-onlyfake/>



Figure 1: Examples of a real ID and popular physical attacks (print, screen and physical composite) available in our proposed FakeIDet2-db. ***Note** - The personal information is redacted in this figure to protect the privacy of the subject.

of international challenges such as DeepID³ (although the evaluation was private and is not publicly available yet) highlighting a considerable gap in performance between using “real” IDs and official ones (i.e., 0.99 vs. 0.71 F1-score for the winner of the challenge). The main reason for considering this “real” scenario is due to privacy concerns, as some fields of the ID contain sensitive information. This is one of the key motivations for the present study, to research possible solutions to previous concerns through the exploration of realistic scenarios in which research institutions can collaborate with, for example, governments or banks to advance in this challenging research direction.

In the present study, we hypothesize that using *patches* from IDs, instead of the whole ID, to train fake ID detectors might provide benefits from both performance and privacy points of view in real-world scenarios. Fig. 2 provides a graphical representation of the current scenario considered nowadays for the problem of fake ID detection (top), versus our proposed privacy-aware proposed scenario (bottom). In both scenarios there are two main actors: *ID Holders* (e.g., government, police, bank, etc.), which provide digital services to citizens and own large-scale datasets of real IDs, and the *AI Researchers* (e.g., research institutions), which have the experience and technology to develop fake ID detectors, but not the data. The current scenario based on sharing the whole ID raises privacy concerns, limiting the development of robust fake ID detectors. Also, there are important concerns in terms of attacks, e.g., if the attackers are able to access to the model trained on whole ID private data, they could use techniques that retrieve the training data with small prior information about

³<https://deepid-iccv.github.io/>

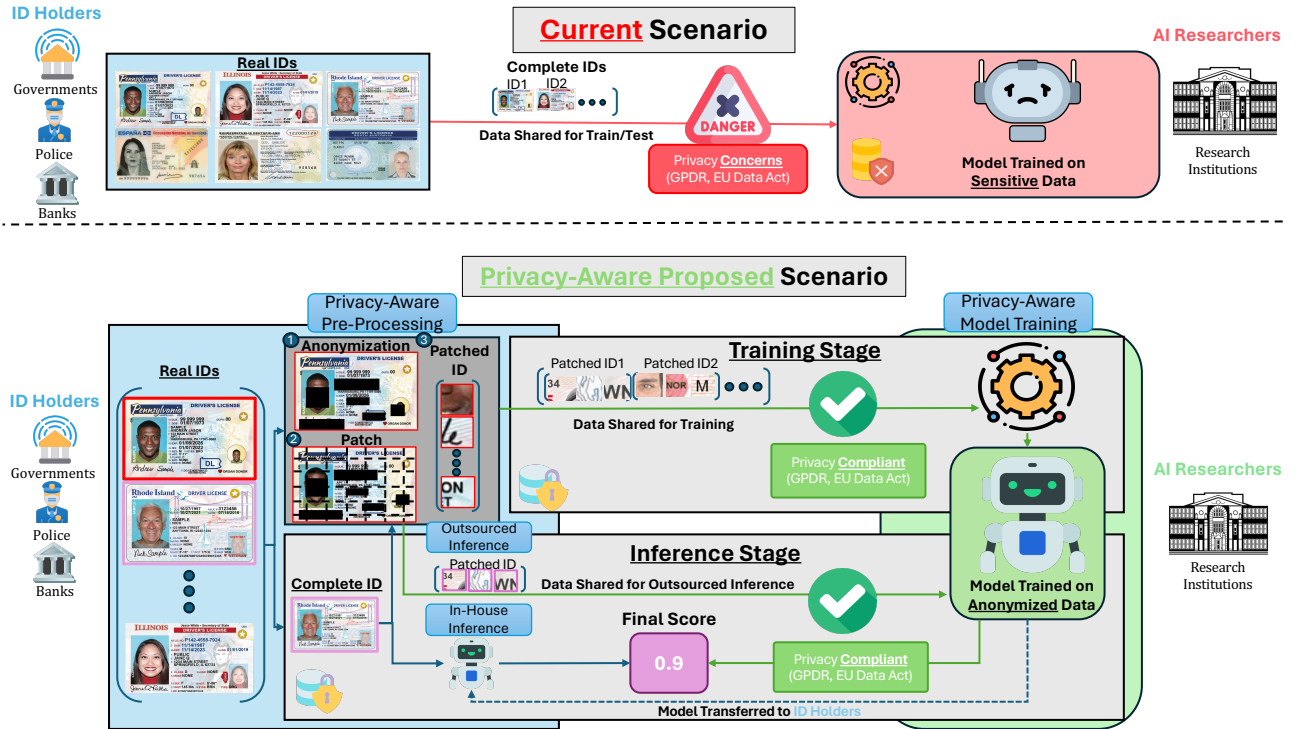


Figure 2: Our proposed framework for privacy-aware fake ID detection. Current scenario (top) carries privacy concerns regarding data regulations, and need for complete ID share between ID Holders and AI Researchers. Our framework proposes an scenario where sequences of non-ordered patches extracted from different levels of anonymized real IDs can be used to preserve ID owners’ sensitive information for data sharing and inference in both in-house or outsourced schemes.

the data distribution [12, 40].

Our proposed privacy-aware scenario is based on the premise that an individual patch contains much less sensitive information than the whole ID. In addition, in order to provide flexibility to the particular restrictions of each ID Holder, we explore different anonymization levels, removing patches from sensitive regions as desired. For example, ID Holders may request AI Researchers to train a fake ID detector but they do not want to share any personal information about the ID owners. As a result, ID Holders can anonymize the sensitive sections from an ID, depending on their preferences for the task at hand, and extract patches from the areas which hold non-anonymized information. Additionally, to increase privacy, the extracted patches can be randomized regarding the order in which they are shared with the AI Researchers, further preventing reconstruction. This flexibility allows a fruitful collaboration between ID Holders and AI Researchers in order to train fake ID detectors under any ID Holder restrictions.

Once the fake ID detector is trained by the AI Researchers, the ID Holders can decide whether inference is carried out inside the AI Researchers infrastructures or internally, as seen in Fig. 2. For example, if the ID Holders want to perform in-house inference using sensitive information that they only have access to, the AI Researchers can transfer the ID Holders the fake ID detector

previously trained using anonymized IDs. However, if the ID Holders do not have such resources, they can rely on the AI Researchers for inference, since the ID Holders always control the amount of sensitive information shared for each ID. The proposed scenario can also be applicable to the research community in order to advance in this challenging topic, since research groups can share patches of IDs, including different levels of anonymization as desired.

The main contributions of the present study are as follows:

- We explore novel approaches in order to facilitate the collaboration between ID Holders and AI Researchers in real-world fake ID detection scenarios. Concretely, instead of feeding the fake ID detectors with the whole ID, as commonly done in the literature, we propose to explore privacy-aware scenarios based on different patch sizes (64×64 and 128×128) and anonymization configurations (non-, pseudo-, and fully-anonymized ID). This proposal increases flexibility to both ID Holders and AI Researchers for both training and inference stages, as shown in Fig. 2. Depending on the particular restrictions of the ID Holder, different setups can be selected to optimize both privacy and performance.
- We provide a novel database, FakeIDet2-db, which contains official real data, along with *print*, *screen*, and *physical composite* attacks. To the best of our knowledge, FakeIDet2-db is the first database containing physical composite forgeries, as previous ones considered digital composites. In total, FakeIDet2-db comprises 922,057 patches extracted from 2,000 ID images (pseudo-, and fully-anonymized configurations) from 47 different Spanish IDs. In addition, in order to increase the variability during the acquisition, we consider three smartphones for different end-users, including different hardware and software: iPhone 15 (high-end), Xiaomi Mi 9T Pro (medium-end) and Redmi 9C NFC (low-end). To add further variability, images are taken at 3 different heights (10 cms, 12.5 cms and 15 cms) with respect to the ID document and also different illumination conditions: *no-light* with the camera flash activated, *dim-light* with/without the camera flash activated and *bright-light* with/without the camera flash activated.
- We propose a novel privacy-aware fake detector, FakeIDet2, which introduces two novel learnable modules: the Patch Embedding Extractor and the Patch Embedding Fusion. The Patch Embedding Extractor leverages DINOv2 foundation model to learn representations of individual patches from real/fake IDs, using an optimized AdaFace loss function [17] through adaptable class-weights, which evolve as the training progresses. Once the embeddings are obtained, they are forwarded jointly into the Patch Embedding Fusion, based on Multi-Head Self-Attention (MHSA) [36], learning relations between patch representations to classify each ID.
- We have developed a standard, reproducible benchmark on which we evaluate the performance of our proposed FakeIDet2 in 3 different ID databases (DLC-2021 [30], KID34K[27], and Benalcazar *et al.* synthetic database from [5]), considering both physical and synthetic attacks, with the goal of assessing the performance in realistic out-of-distribution data. The proposed FakeIDet2-db and benchmark will be publicly available for

reproducibility reasons in our GitHub repository⁴, allowing a straightforward comparison of recent approaches with the state of the art.

A preliminary analysis of this privacy-aware scenario was conducted in [23]. The present article significantly improves [23] in the following aspects: *i*) we present our novel publicly available FakeIDet2-db, which increases the number of unique real IDs (47 subjects) along with more acquisition devices (3), illumination (3) and height (3) conditions, resulting in 922,057 patches extracted from 2,000 ID images (pseudo-, and fully-anonymized configurations); *ii*) we include physical composite attacks in our novel FakeIDet2-db. To the best of our knowledge, this is the first database that includes this kind of Presentation Attack Instrument (PAI); *iii*) we propose a novel approach for fake ID detection, FakeIDet2, that overcomes the limitations regarding patch-level fusion encountered in FakeIDet [23]. While FakeIDet performs a simple mean of scores assigned to each individual patch for IDs level prediction, FakeIDet2 comprises two learnable modules (i.e., Patch Embedding Extractor and Patch Embedding Fusion) to leverage the fusion of learned patch representations, depending on the visual characteristics from real/fake IDs. The representations at patch level are obtained through an optimized version of AdaFace [17], including dynamic class weights, which accounts for the severe class imbalance present in the databases for the different PAIs. The fusion of the representations is performed via MHSA, which ponders the embeddings values based on the relations between them, to then compress them into a single embedding, via attention pooling based on [4]. The impact of these improvements can be seen in the results (Sec. 6); and *iv*) in order to advance in this research field, we propose a standard public benchmark considering a wide variety of physical and synthetic attacks from different databases in the literature, allowing a direct comparison of recent approaches with the state of the art.

The rest of the paper is organized as follows. Sec. 2 provides an overview of the fake ID detection problem. In Sec. 3 we present our FakeIDet2-db, delving into the acquisition process for capturing real IDs and their fake counterparts. Sec. 4 introduces our novel privacy-aware fake detection method, FakeIDet2. Sec. 5 proposes a reproducible experimental protocol and standard benchmark, considering experiments in both intra- and cross-database scenarios. Finally, Sec. 6 analyzes the performance of our proposed fake detector using the proposed experimental protocol and standard benchmark and Sec. 7 draws the final conclusions.

2. Related Work

This section provides an overview of the fake ID detection problem. Sec. 2.1 provides a revision of databases considered in the field. Sec. 2.2 focuses on representative fake ID detectors and recent international challenges. Finally, we summarize key aspects in Sec. 2.3.

2.1. Databases

Table 1 provides a summary of the most relevant public/private databases in the field of fake ID detection. One of the first family of databases was

⁴<https://github.com/BiDALab/FakeIDet2-db>

Database	#Samples	#IDs	#Devices	#PAIs	Official Real IDs?	Public?
BID (2020) [32]	28,800	28,800	N/A	8	✗	✓
DLC-2021 (2021) [30]	1,424 (videos)	1,000	2	4	✗	✓
Mudgalgundurao <i>et al.</i> (2022) [22]	97,477	433	N/A	2	✓	✗
Benalcazar <i>et al.</i> (2023) [5]	3,000	3,000	Synthetic	1	✗	✓
KID34K (2023) [27]	34,662	92	12	3	✗	✓
IDNet (2024) [39]	837,060	837,060	Synthetic	7	✗	✗
Open-Set (2024) [19]	5,424	N/A	Synthetic	2	✗	✓
Gonzalez <i>et al.</i> (2025) [13]	190,000	190,000	N/A	5	✓	✗
FakeIDet-db (2025) [23]	90	30	1	2	✓	✓
FakeIDet2-db (proposed)	2,000	47	3	3	✓	✓

Table 1: Summary of private and public databases considered in the literature. For completeness, we also indicate whether the databases used to train fake ID detectors are available or not for public research.

the MIDV-family [1, 8, 7]. With the original purpose of Optical Character Recognition (OCR), Bulatov *et al.* synthetically created a set of physical fake ID, passports and driving licenses. They used several digital templates from multiple countries which they filled with names and addresses from Wikipedia and artificially generated faces. As different versions from the database were released, the number of fake samples were increased. DLC-2021 database [30] used the documents of the MIDV-family to create PAIs: *color print*, *gray print* and *screen*. The authors also provided “real” samples, although they should be considered fake samples as they are just high-quality prints built by them, not official ID. A similar work is presented in the KID34K dataset [27], where Park *et al.* introduced a dataset of 34,000 images from 82 Korean IDs and driving licenses. As in the MIDV-family, the authors claimed to release “real” samples, but they were also built by the authors, not official documents. In order to prove the quality of the “real” samples, they trained a Convolutional Neural Network (CNN) using the KID34K dataset, forwarding the whole ID. Evaluation was performed using both official Korean IDs and “real” documents. After that, the authors applied a dimensionality reduction technique to visualize the model’s embeddings in 2D, where they showed that embeddings from both official and “real” generated IDs from the KID34K database were similarly distributed in the embedding space. These results raise questions regarding security in the fake ID problem, since fake IDs may be generated with such resemblance to real ones, that deep-learning models may not be able to extract distinguishable features for proper PAD. Soares *et al.* [32] introduced the Brazilian Identity Document (BID) database with a total of 28,800 images from Brazilian IDs that have been digitally altered via different algorithms that remove, blur and replace different personal information from the real IDs, to comply with data

privacy regulations. In [13], Gonzalez and Tapia proposed a more sophisticated attack procedure, i.e., printing the digital copy over a Poli-Vinyl Chloride (PVC) card, which resembles even more the appearance of real IDs.

Regarding synthetic data, Benalcazar *et al.* proposed in [5] to use Generative Adversarial Networks (GANs) to produce synthetic Chilean IDs. The proposed GAN was trained using only real Chilean ID samples. Although the data synthesized by the authors is not strictly real, this was presented as a good idea to cover partially the lack of real data, e.g., as a data augmentation strategy in training. Another synthetic database is IDNet [39], where Xie *et al.* proposed a database that comprises synthetic copies of IDs from 10 countries and 10 states from the United States of America. Given an ID template, portrait images and data from the owners were synthetically generated, with special care that the fields matched with the gender and age of the synthetic portrait image. Additionally, the authors created six different types of digital manipulations, including inpainting, field cropping or face morphing. A total of 837,060 IDs were generated, making it the biggest and most diverse to this day, although no real data is included. Markham *et al.* [19] developed Open-Set, a database that leverages neural style transfer, via GANs-based models to transfer textures from *print* and *screen* attacks to “real” images from the MIDV-2020 and DLC-2021 databases, creating even more samples of attacks.

2.2. Fake ID Detection Methods and International Challenges

One of the first methods was presented in [22], where the authors trained a CNN via pixel-wise classification using an in-house database, reporting a 2.22% EER. Gonzalez and Tapia proposed in [13] a two-stage system which first used a neural network to evaluate if the submitted ID is real or fake, evaluating digital PAIs of type *composite* or *synthetic*. The second network classified the submitted ID between real or fake, evaluating physical PAIs such as *print*, *display* or *PVC*. When concatenating both systems, the Bona-fide Presentation Classification Error Rate at a fixed decision threshold $\tau = 0.01$ ($BPCER_{100}$) is 0.92%.

Evidences that the fake ID detection field is receiving increasing attention in the last years is the organization of international challenges in top conferences. The first challenge was introduced at IEEE IJCB 2024 [33]. No data was given by the organizers, and the submitted fake ID detectors were evaluated over real IDs, which further reduced the model’s performance, since the winner of the challenge achieved an EER of 21.87%. The second edition of this challenge has been hosted at IEEE IJCB 2025⁵, where the organizers proposed two tracks. The first track considered IDs created by the organizers using PVC cards as “real” documents and the rest as attacks, and the second track treated only official IDs as real. Only for the first track, a database was given to the participants. The winner for the first track reported an EER of 11.34%, while for the second track, the best team reported an EER of 6.36%, but the second and third teams reported EERs of 23.87% and 31.94%, respectively. These results showcase this is a challenging task, specially due to the lack of public real data. Recently, the first challenge including digital manipulations for fake ID detection has been organized at IEEE/CVF ICCV 2025⁶. This challenge proposed

⁵<https://sites.google.com/view/ijcb-pad-id-card-2025/>

⁶<https://deepid-iccv.github.io/#home>

two tracks, one for binary classification, which focused on PAD (i.e., detecting fake and real documents) and one for localization (i.e., providing a mask that showed the tampered sections). The organizers provided a database for all participants, named FantasyID, which contained fake templates of different countries from different regions of the world. The “real” ID data was created by printing high-quality fakes using PVC cards, and taking images from them. After that, those images were digitally altered through face-swapping and text inpainting methods. For the detection track the evaluation was performed using the F1-score with a decision threshold fixed to $\tau = 0.5$ over two datasets: the FantasyID evaluation set, which contained PAIs which were not available in the training set, and a private dataset which was provided by the company PXL Vision, with the same type of attacks as in the FantasyID dataset, but using official IDs as real. The final score, denominated Aggregated F1-score, was a pondered mean that gave more importance to the F1-score obtained over the private dataset, hence, benefiting models that generalized better to out-of-distribution data. The winning team achieved an Aggregated F1-score of 0.8, obtaining a F1-score of 0.99 and 0.72 in both the FantasyID dataset and private dataset, respectively. These results, although impressive, show that there is a present issue in domain adaptation between official real IDs and fake samples created in laboratory conditions that are considered “real”. Hence, providing privacy preserving mechanisms that allow to share official real IDs without compromising individual’s personal information is fundamental to further advance in this research field.

2.3. State-of-the-Art: Summary

A clear trend can be observed based on previous sections. Public databases in the literature do not have official real data available, and fake ID detectors trained using private databases with real data do not release neither the code nor the weights to the research community, making impossible to perform fair comparisons among state-of-the-art methods. Moreover, the characteristics of those databases are not always detailed (e.g., acquisition devices or number of unique IDs), which make even more difficult to advance in the field. The present study aims to advance through the following key contributions: *i*) the release of a novel database, FakeIDet2-db, increasing the number of images from real and fake IDs, *ii*) the inclusion of a new kind of PAIs, named *physical composite*, to the proposed database, being the first one that contains this kind of attack, *iii*) a novel method for privacy-aware fake ID detection based on fusion of representations from individual patches, and *iv*) a novel standard public benchmark that considers a wide variety of physical and synthetic attacks included in other public databases in the literature, considering IDs with different templates and demographic regions.

3. Proposed Database: FakeIDet2-db

This section describes our novel FakeIDet2-db. Concretely, Sec. 3.1 and Sec. 3.2 provide all the details of the real and fake ID acquisition, whereas Sec. 3.3 describes the post-processing carried out for the different anonymization and patch size configurations.

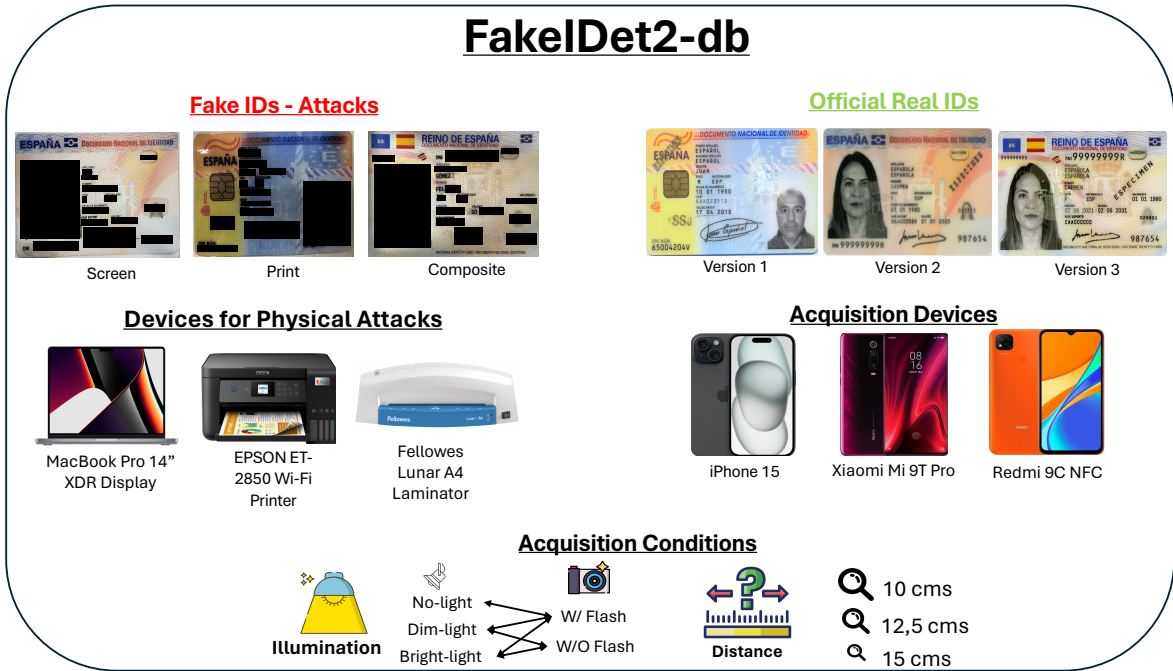


Figure 3: Main characteristics of our proposed public FakeIDet2-db. **Note* - For the Fake IDs - Attacks, the personal information is redacted in this figure to protect the privacy of the subjects. Official Real IDs are based on non-real examples.

3.1. Acquisition Setup: Real IDs

Fig. 3 summarizes the main characteristics of our proposed public FakeIDet2-db. Regarding the number of unique IDs, our database comprises 47 different official Spanish IDs. Spanish electronic IDs appearance have changed during the years, which is a key aspect that has also been considered while capturing this database, including three different versions. For the acquisition, we used three different smartphone models (Apple iPhone 15, Xiaomi Mi 9T Pro and Redmi 9C NFC), aiming to cover the range of sensor quality from high-end to low-end, respectively. Their main technical specifications are provided in Table 2 where we can see that both iPhone 15 and Mi 9T Pro have main camera sensors with 48MP while the Redmi 9C NFC only has 13MP. The iPhone camera is the best one in terms of adaptability to low light scenarios, given its aperture of $f/1.6$, although Mi 9T Pro is close with an aperture of $f/1.75$. However, the Redmi 9C NFC struggles in these kind of low-light scenarios, given that its aperture is greater, $f/2.2$. Regarding image resolution, the iPhone 15 is able to shoot ProRes images up to 8K resolution, but for our acquisition process, we set it to 4K, since both Mi 9T Pro and Redmi 9C NFC can only shoot images at that resolution. Pictures of IDs were taken using a 4:3 aspect ratio. Three different heights were considered with respect to the document's vertical: 10 cms, 12.5 cms and 15 cms, building a 3D printed adjustable platform. This enabled acquiring IDs precisely, similar to [22], where they captured IDs using a mobile application that provided a template in the camera preview to match where the IDs borders should be when the picture was taken.

In order to provide more variability, we also considered different light condi-

Feature	iPhone 15	Mi 9T Pro	Redmi 9C NFC
Main Sensor	48 MP (1/1.28")	48 MP (1/2")	13 MP (1/3.1")
Aperture	$f/1.6$	$f/1.75$	$f/2.2$
Resolution	4,032×3,024	4,032×3,024	4,032×3,024
ISP / SoC	Apple A16	Snapdragon 855	Helio G35
Pixel Size	1.22 μm /2.44 μm	0.8 μm /1.6 μm	1.12 μm

Table 2: Technical specifications of the smartphones considered in FakeIDet2-db.

tions in terms of room illumination: *i) no-light*, with the camera flash activated, *ii) dim-light*, with images taken with/without the camera flash activated, and *iii) bright-light*, with images taken with/without the camera flash activated.

Therefore, given the aforementioned variability factors, for a unique ID, we obtained 45 images (i.e., 3 smartphones \times 3 heights \times 5 light-conditions) covering different conditions, yielding a total of 2,115 (i.e., 47 \times 45) images of real IDs.

3.2. Acquisition Setup: Attacks

Fig. 1 shows visual examples of the physical attacks (print, screen and physical composite) available in our proposed FakeIDet2-db. Note that the personal information is redacted in the figure of the article to protect the privacy of the subject.

To manufacture the print attacks, we used a HP ScanJet 8270 scanner at 600 Dots Per Inch (DPI), creating a digital copy of the real ID. After that, we printed the fake IDs using an EPSON ET-2850 Wi-Fi printer and laminated them to improve the realism using a Fellowes Lunar A4 thermal laminator, providing print attacks with the characteristic glossy texture from real IDs. The acquisition process was the same as for the real IDs, yielding a total of 2,115 images for print attacks.

For screen attacks, we used a MacBook Pro 14" XDR screen, where the 2,115 images of real documents were displayed in full-screen and covering the whole smartphone camera preview. To increase variability across smartphone devices, each image was displayed and then captured using one randomly selected smartphone, ensuring that approximately one-third of the images were taken with each device.

Regarding the physical composite attacks, we cut sensitive sections from print attacks and placed them over the sensitive areas of real IDs. Regarding privacy considerations, we only cut the date of birth, the name and both surnames from the ID owner along with partial sections of the ID's number. To provide even more variability, some physical composite attacks were created using cut-outs from several print attacks. The cut-outs of sensitive sections from a print attack were never displayed at the same time, further protecting the ID owner's sensitive information. Additionally, we did not use the ID owner's portrait image, as it is sensitive information which cannot be shared by any circumstances. After that, we captured composite attacks following the same procedure as for real IDs, described in Sec. 3.1, balancing the number of images of real and all types of attack across the database to 2,115.

Gathering all images from real and fake IDs, our database contains 8,460 total IDs images. From them, we selected 1,000 images, balancing them across



Figure 4: Examples of the different anonymization levels considered in the present study.

different types of attacks and bona fide data (250 samples per class), different capture devices, and different illumination and height conditions. This sub-sampling aimed to avoid including images of real and fake IDs under all acquisition conditions, ensuring that fake ID detectors do not rely on superficial cues, such as illumination patterns, to distinguish between real and fake IDs, which could lead to overfitting [16].

3.3. Post-Processing: Anonymization and Patch Extraction

Fig. 4 provides graphical examples of the different anonymization configurations explored in the present study in order to facilitate the collaboration between ID Holders and AI Researchers in real-world fake ID detection scenarios. The criteria followed to remove sensitive information at each anonymization configuration is the following:

1. *Non-Anonymized*: no sensitive sections are anonymized, so all information is available to detect real/fake IDs.
2. *Pseudo-Anonymized*: partial sections with sensitive information of real/fake IDs is displayed. This kind of anonymization is consistent along all images from a same ID, so no reconstruction is permitted.
3. *Fully-Anonymized*: all sensitive sections of real/fake IDs are completely anonymized.

Referring to *pseudo*- and *fully*- anonymized configurations, we used EasyOCR⁷ and GNU Image Manipulator Program (GIMP) to cover the sensitive regions with pitch black rectangles (with the color code (0,0,0) in the RGB spectrum). Since we had two levels of anonymization applied to the original, non-anonymized images, we obtained 2,000 images of real and fake IDs. Given that we had several images taken from the same ID, we took special care in covering the same partial sensitive sections across every image in the pseudo-anonymized configuration. Once all the IDs were anonymized, we processed them and extracted patches using PyTorch’s `unfold` method, specifying the same step and stride size as the patch size, to avoid overlapping. Patches with over 80% of pitch black content were discarded and the remaining ones were kept with a sampling probability of $p = 0.9$, to further prevent reconstruction. After that, for each ID image, we created a folder where the extracted patches were stored using random numbers of six figures as the filename for patch (i.e., 762542.jpeg), so no spatial layout could be inferred.

⁷<https://github.com/JaidedAI/EasyOCR>

		Real	Print	Screen	Composite
Patch Size	Anon. Level				
128×128	Non-Anon	56,017	52,976	55,927	3,810
	Pseudo-Anon	32,875	28,432	32,170	1,805
	Full-Anon	21,896	20,363	21,474	1,216
64×64	Non-Anon	222,622	211,396	221,610	7,931
	Pseudo-Anon	152,612	132,920	148,599	6,297
	Full-Anon	110,162	101,178	107,104	2,954

Table 3: Number of patches per real/fake ID, patch size, and anonymization level considered in our proposed FakeIDet2-db.



Figure 5: Graphical samples of real/fake patches extracted from different IDs. Real patches (first column, green color), are shown along the different types of attacks in the proposed database (second, third, and fourth columns, red color), at both 128×128 and 64×64 sizes.

An important point is the amount of patches available regarding anonymization and patch size configurations, which are depicted in Table 3 for real IDs and the different attacks considered. For instance, the Full-Anon, 128×128 configuration shows a noticeable drop in terms of number of patches compared to the Non-Anon, 64×64 configuration, having almost ten times less amount of patches. As we plan to release the FakeIDet2-db, the pseudo- and fully-anonymized ID configurations at 128×128 and 64×64 patch sizes will be available for privacy reasons, proving in the results section (Sec. 6) that these privacy-aware scenarios are very useful to facilitate collaborations between ID Holders and AI Researchers. If we consider the number of patches from said configurations, a total of 922,057 patches extracted from 2,000 images will be available for researchers to train and benchmark their proposed fake ID detectors.

For completeness, Fig. 5 shows different examples of real/fake patches extracted from different IDs. One can see that the 128×128 patch size contains much more information compared to their 64×64 counterparts. Some small traces can be observed in the different attacks. For instance, the composite attacks might show the change of color and texture between the background and the altered section at the foreground. On the other hand, patches from the screen attacks might show subtle traces of the characteristic Moiré patterns.

4. Proposed Method: FakeIDet2

Our proposed fake ID detection method, FakeIDet2, proposes a privacy-aware, patch-level representation fusion. Fig. 6 provides a graphical representation of FakeIDet2. This comprises three main modules: the Privacy-Aware Patch Extractor, the Patch Embedding Extractor, and the Patch Embedding Fusion. The Privacy-Aware Patch Extractor module receives a complete ID, considering any anonymization level presented in Sec. 3.3. This first module divides the whole ID into patches, removing sensitive information if applicable (i.e., regions of the ID that are blacked out). After that, those patches are forwarded into the Patch Embedding Extractor, which uses a fine-tuned DINOv2 as a feature extractor to learn discriminative features at patch-level from each type of PAI, providing an embedding for each patch. Then, those embeddings are treated as tokens, and passed into a MHSA layer, which ponders the embeddings values depending on their importance in the sequence. After that, an attention pool layer selects discriminative features from the sequence, obtaining a single embedding, which is forwarded to a Multi-Layer Perceptron (MLP) that yields a final score per ID, indicating whether is real or fake. We describe next the technical details of the *learnable* modules of FakeIDet2.

4.1. Patch Embedding Extractor

To learn features at patch level effectively, we go deep into representation learning [6, 25, 9], aiming to obtain compressed, meaningful representations from high-dimensional data into the embedding space. To do so, we treat patches coming from both real and fake IDs as four different classes (i.e., 3 PAIs + real) and use DINOv2’s (ViT-S/14) [26] backbone with its weights frozen. Using DINOv2 for extracting patch embeddings seems appropriate, since the goal for its original training procedure was to match the embedding distribution between images where the full context is given and random patches extracted from the same image. To leverage these features, we attach a final layer to DINOv2 embeddings, hence, our Patch Embedding Extractor is defined as an encoder function that maps an input patch $x_i \in \mathbb{R}^{p \times p \times c}$, where p is the patch size and c is the channel dimension (i.e., $c = 3$ in the RGB spectrum), to its corresponding compressed representation $z_i \in \mathbb{R}^d$, where d is the dimension of the embedded space.

We explore several softmax-based loss functions, i.e., CosFace [38], ArcFace [10], and AdaFace [17], to assess which one suited our problem best for discriminative representation learning. The generic formulation for the Softmax loss function is defined in Eq. 1, where C is the number of classes and $f(\theta_{y_i})$ is a function that computes the alignment between the embedding obtained from the input image and the class prototype of its label y_i . Hence, the objective for an embedding of one class is to be as close as possible to other embeddings from the same class (better aligned) while being apart from embeddings of other classes by an imposed distance, called margin (worst aligned). The main differences between these loss functions reside in how the margin is computed for the alignment function, $f(\theta_{y_i})$. For example, CosFace, defined in Eq. 2, computes the loss by adding the margin m to the cosine similarity, while ArcFace, defined in Eq. 3, computes the loss by adding an angular margin m to the cosine similarity. In the case of AdaFace, defined in Eq. 4, the margin is computed adaptively, depending on the image quality, which is computed as the norm of

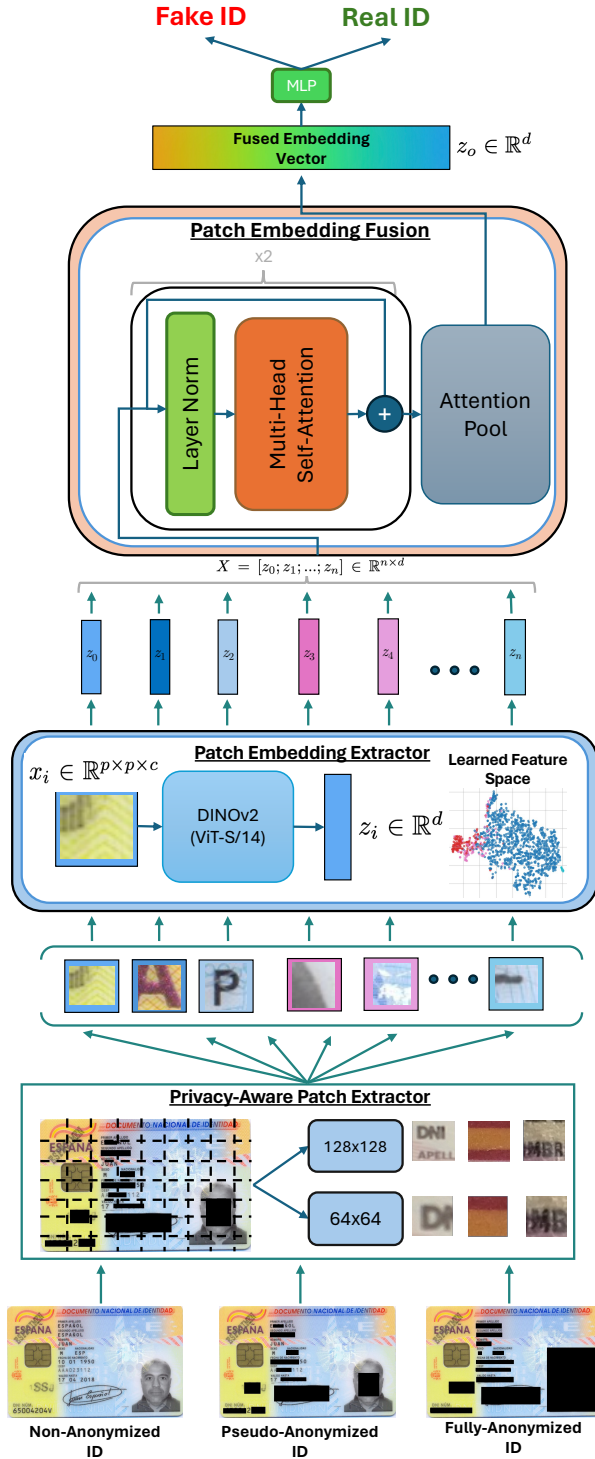


Figure 6: Description of our proposed fake ID detector, FakeIDet2. Our proposal has three different stages: *i*) the whole ID is forwarded to the Privacy-Aware Patch Extractor, extracting patches at fixed size (128×128 or 64×64); *ii*) those patches are forwarded into the Patch Embedding Extractor, which yields an embedding per patch; and *iii*) finally, those embeddings are used at the Patch Embedding Fusion module to generate a single embedding which is used by a MLP, providing a final score.

embedding obtained from the input image, which is normalized based on batch statistics for better stability, which is denoted by $\|\hat{z}_i\|$.

$$\mathcal{L} = \log \left(\frac{\exp(f(\theta_{y_i}))}{\exp(f(\theta_{y_i})) + \sum_{j \neq y_i}^C \exp(s \cos \theta_j)} \right) \quad (1)$$

$$f(\theta_{y_i})_{\text{CosFace}} = \begin{cases} s \cos(\theta_j - m) & j = y_i \\ s \cos(\theta_j) & j \neq y_i \end{cases} \quad (2)$$

$$f(\theta_{y_i})_{\text{ArcFace}} = \begin{cases} s \cos(\theta_j + m) & j = y_i \\ s \cos(\theta_j) & j \neq y_i \end{cases} \quad (3)$$

$$f(\theta_{y_i})_{\text{AdaFace}} = \begin{cases} s \cos(\theta_j + (-m \cdot \|\hat{z}_i\|)) - (m \cdot \|\hat{z}_i\| + m) & j = y_i \\ s \cos(\theta_j) & j \neq y_i \end{cases} \quad (4)$$

One issue that we encountered when training the Patch Embedding Extractor was that softmax-based loss functions did not account for the severe class imbalance in the physical composite attacks (see Table 3). To address this limitation, we propose to apply dynamic class weights to these loss functions, which evolve as the training progresses. The initial weights $w_0 \in \mathbb{R}^C$, where C is the number of classes, are computed as the normalized inverse of the frequency for each class using Eq. 5, where N is the total number of patches in the database, and N_i is the total number of patches belonging to the i -th class.

$$w_0 = \begin{bmatrix} \frac{N}{N_1} \\ \frac{N}{N_2} \\ \dots \\ \frac{N}{N_C} \end{bmatrix} \times \sum_{i=1}^C \frac{C}{N_i} \quad (5)$$

After that, the class weights are updated at each epoch until they all converge to 1, hence, giving progressively the same weight to all classes. The update rule is presented in Eq. 6, where $w_t \in \mathbb{R}^C$ is a vector that stores the class weights at time-step t , $\mathbf{1} \in \mathbb{R}^C$ is a vector full of ones, $\lambda_t \in [0, 1]$ is a pondering factor that linearly decays from 1 to 0 as training progresses, and e is the total number of time-steps involved in the training procedure. Intuitively, at the beginning of the training, the class weights are going to be close to w_0 giving more importance to the under-represented class, but, as time-steps go by, the class weights are going to get closer to 1, giving all classes the same importance by the end of the training.

$$w_t = (1 - \lambda_t)\mathbf{1} + \lambda_t w_0, \quad \lambda_t \leftarrow \lambda_0 + (\lambda_e - \lambda_0) \times \left(\frac{t}{e}\right) \quad (6)$$

These class-weights are then used to modulate the gradient signal that the margin loss function produces, giving higher values when the embeddings from

the underrepresented class are close to the embeddings from another class. The modified version of this loss is defined in Eq. 7, where \mathcal{L} is the loss function defined in Eq. 1, w_{t,y_i} is the class weight associated to the label y of the i -th element of the batch at epoch t .

$$\mathcal{L}_{\text{weighted}} = -w_{t,y_i} \cdot \mathcal{L} \quad (7)$$

4.2. Patch Embedding Fusion

To effectively fuse all patch embeddings of a given ID, we make use of the MHSA layer presented in the Transformer architecture [36]. This mechanism was introduced to solve issues related to model long-range dependencies, which are typical in Recurrent Neural Networks (RNN) models, which process information sequentially. However, in the Self-Attention mechanism, all the elements of the input sequence are processed at the same time, enabling modeling dependencies from tokens that are from afar. The Self-Attention layer expects as input a sequence of embeddings (or tokens) $X \in \mathbb{R}^{n \times d}$, where n is denoted as the sequence length and d the embedding dimension. The sequence is processed according to the Self-Attention mechanism, defined in Eq. 8, where Q is the query, K is the key, V is the value, and d_k is the projected embedding dimension for the query and the key. The query, key and value matrices are single linear projections from X , which are computed as $Q = XW_Q$, $K = XW_K$ and $V = XW_V$, respectively, where $W_Q \in \mathbb{R}^{d \times d_k}$, $W_K \in \mathbb{R}^{d \times d_k}$ and $W_V \in \mathbb{R}^{d \times d_v}$, where d_v is the projected dimension for the value. Hence, the obtained sequence after the Self-Attention mechanism is a matrix $X' \in \mathbb{R}^{n \times d}$ where each token values have been modified depending on their importance in the sequence, compared to their peers.

$$\text{Attention}(Q, K, V) = \text{softmax} \left(\frac{QK^\top}{\sqrt{d_k}} \right) V \quad (8)$$

Furthermore, the attention mechanism allows the queries, keys, and values to be linearly projected h times using different learned projections of dimensions d_k and d_v . To achieve this, d_k and d_v are typically set to d/h , where d is the model dimension. Each of these computations defines an attention head (Eq. 9). The outputs of the h attention heads are concatenated and projected back to the original input dimension using a final linear transformation $W^O \in \mathbb{R}^{hd_v \times d}$ (Eq. 10).

$$\text{head}_i = \text{Attention}(Q_i, K_i, V_i) \quad (9)$$

$$\text{MultiHead}(Q, K, V) = [\text{head}_1, \dots, \text{head}_h]W^O \quad (10)$$

Since the Patch Embedding Extractor produces an embedding z_i for each patch x_i , we treat the set of patches that come from a single ID as a sequence $X = [z_0; z_1; \dots; z_n] \in \mathbb{R}^{n \times d}$, where n is the number of patches from a single ID

and d is the dimension from the embedding obtained from the Patch Embedding Extractor. These embeddings are then normalized via layer normalization [3] and forwarded into the MHSA layer, that produces a feature sequence $X' = [z'_0; z'_1; \dots; z'_n] \in \mathbb{R}^{n \times d}$ where the embeddings values z'_i have been modified according to their importance in the input sequence. Additionally, we leverage residual connections [14] to enable better gradient flow in the training procedure, as two layers of MHSA and layer normalization are stacked together in this module, where the first MHSA layer has $h = 8$ attention heads and the second layer has $h = 4$ attention heads.

Using the MHSA mechanism is beneficial for our proposed FakeIDet2 as: *i)* it leverages the patch embedding space learned by the Patch Embedding Extractor, and *ii)* it can detect elements of the sequence that may be anomalous, which is analogous to detecting tampered sections of a composite attack. Then, the feature sequence is forwarded into a temporal attention pool module, similar to [4], generating a single embedding $z_o \in \mathbb{R}^d$. Finally, we use z_o as an input to an MLP, comprising a single layer with sigmoid activation, obtaining a final score per ID.

5. Experimental Setup

In order to define a standard, reproducible benchmark that allows to advance properly in this research field, in this section we define our experimental setup. First, Sec. 5.1 describes the specific hyperparameters of our proposed FakeIDet2 method. Then, in Sec. 5.2 we describe the experimental protocol and the different scenarios of interest in the analysis. Finally, Sec. 5.3 describes the evaluation metrics. As a general note, we use the EER metric as a performance indicator to obtain the best patch and anonymization configuration. For all training procedures and experiments, we used only one NVIDIA RTX 3080 with 10GB of VRAM.

5.1. FakeIDet2: Hyperparameters

Regarding the Patch Embedding Extractor, for any patch size the input is resized to 224×224 , which is the input shape of DINOv2, with an embedding layer of dimension $d = 128$. We use Adam optimizer with weight decay, an initial learning rate $\alpha_0 = 0.00125$, and exponential decays for the momentum estimators of $\beta_1 = 0.9$ and $\beta_2 = 0.999$, respectively, and a weight decay $\delta = 0.0001$. All models are trained for 70 epochs, using the modified versions of the softmax-based losses presented in Sec. 4.1 with an early stopping condition that ends the training if the loss in the validation does not decrease for 5 consecutive epochs. Additionally, we use a cosine annealing decay scheduler for the learning rate, with values decreasing from $\alpha_0 = 1.25e - 3$ to $\alpha_e = 1.25e - 4$, and a batch size of 256. Regarding data transformations, we opt to randomly apply Gaussian blur with a kernel size $k = 3$ and color jitter with a brightness of 0.2, a hue of 0.05, a contrast of 0.25, and a saturation of 0.2. These data transformations are applied in training time with a probability of $p = 0.2$. Finally, the pixel values are normalized according to ImageNet mean and standard deviation statistics.

For the Patch Embedding Fusion, in particular the MHSA layers, we define a context length of 384 for both patch configurations, which is enough so that no patch from an ID is left out when performing a forward pass. Furthermore,

we use masked-MHSA to indicate which embeddings should be attended, so that in case the number of patches from a single ID is fewer than the context length, the introduced padded embeddings are ignored. We use Binary Cross Entropy (BCE) loss with class weights, since there is a class ratio of 3 to 1 between fake and real data. For all of our experiments, we choose Adam as the optimizer, using an initial learning rate $\alpha_0 = 1.25e - 4$ and exponential decays for the momentum estimators of $\beta_1 = 0.9$ and $\beta_2 = 0.999$, respectively, with 1 epoch of learning rate warm-up. Additionally, the learning rate followed a cosine annealing decay from $\alpha_0 = 1.25e - 4$ to $\alpha_e = 1.25e - 5$.

All configurations in terms of anonymization levels and patch sizes are trained for 10 epochs with a batch size of 4, selecting the best performing model for each training procedure according to the lowest validation loss achieved.

5.2. Experimental Protocol

In order to assess the feasibility of our proposed FakeIDet2 detector and privacy-aware scenarios to facilitate the collaboration between ID Holders and AI Reseachers, we propose a novel experimental protocol that aims to: *i*) evaluate FakeIDet2 performance regarding patch size and anonymization configurations in our novel FakeIDet2-db, comparing the results with the traditional case in the literature, i.e., feeding the fake detectors with the whole non-anonymized ID, and *ii*) explore domain adaptation, by evaluating FakeIDet2 detector on popular databases in the topic of fake ID detection.

First, in all experiments that involve any kind of training procedure, the database is divided into a development set (80% of the real and fake IDs) and a final evaluation set (the remaining 20%) for all training scenarios. This split simulates a realistic scenario in which the evaluation involves unseen identities. In addition, for our FakeIDet2-db, the first version of the Spanish ID is included only in the final evaluation set, not in the development set, in order to analyze the generalization ability of FakeIDet2 to other ID templates.

Regarding the experiments included in Sec. 6, we first validate the technical details of our proposed FakeIDet2 in terms of performance and privacy. Sec. 6.1 explores the different softmax-based loss functions for representation learning, which will determine the best loss function for the Patch Embedding Extractor module. After that, an exploration in terms of the optimal patch size is conducted in Sec. 6.2, to test whether more patches at lower sizes (i.e., 64×64) yield better performance compared to fewer patches of greater size (i.e., 128×128). Additionally, we also compare the performance of our proposed FakeIDet2 in terms of anonymization levels in Sec. 6.3, which also goes deep into interesting scenarios such as how well a model trained on fully-anonymized data performs on non-anonymized data. Finally, for completeness, we compare FakeIDet2 with our previous FakeIDet [23]. From this set of experiments we will select the best configuration from FakeIDet2 in terms of privacy versus performance.

Then, after validating the technical contributions of FakeIDet2, we analyze its generalization capabilities against unseen scenarios, including leave-one-out experiments for two interesting scenarios: novel attack detection and out-of-distribution sensors. In this case, we train FakeIDet2 with the optimal configuration, leaving either images belonging to one PAI or images taken from one sensor out of the training data, testing the performance of FakeIDet2 when exposed to unseen attacks, or images taken from acquisition devices with sensors

that were not used during training. The analysis of these scenarios are available in Sec. 6.4 and Sec. 6.5, respectively.

Finally, we evaluate in Sec. 6.6 the best configuration of FakeIDet2 in a cross-database scenario, providing a standard public benchmark to the research community. This scenario intends to evaluate our proposed model using unseen databases, where IDs are from different countries, including different templates, and are acquired under different conditions in terms of illumination and acquisition devices. Also, these databases contain different PAIs compared to our proposed database. With this goal in mind, we select three different databases for performance evaluation, DLC-2021 [30], KID34K [27] and Benalcazar *et al.* [5]. These databases are selected for the following reasons: *i*) each database has ID images from three different regions of the world (i.e., Europe, Asia and South America), hence the evaluation is conducted on different distributions in terms of ID templates with different alphabets, and *ii*) we contemplate physical attacks as well as synthetic attacks in our evaluation, to assess the performance of FakeIDet2 to synthetic data in the form of fake IDs.

5.3. Evaluation Metrics

Similar to previous approaches presented in the literature [33], we adopt the ISO/IEC 30107-3 standard⁸ for the evaluation of fake ID detection technology. This includes the use of the Bona-fide Presentation Classification Error Rate (BPCER) and Attack Presentation Classification Error Rate (APCER) metrics. The BPCER (Bona Fide Presentation Classification Error Rate), Eq. 11, where N_{BF} is the number of bona fide samples, RES_i is a term that is equal to 1 if the presented sample is incorrectly classified as an attack, and τ is the operational point, which is a mere threshold used to classify a sample as bona fide if the confidence of the prediction goes below and as an attack if it goes over said value. These measures the proportion of bona fide samples (i.e., real IDs) that are incorrectly classified as attacks (i.e., fake IDs).

$$BPCER(\tau) = \frac{\sum_{i=1}^{N_{BF}} RES_i}{N_{BF}} \quad (11)$$

Conversely, the APCER (Attack Presentation Classification Error Rate), Eq. 12, quantifies the proportion of attack samples (i.e., fake IDs) that are misclassified as bona fide (i.e., real IDs).

$$APCER(\tau) = \frac{1}{N_{BF}} \sum_{i=1}^{N_{BF}} 1 - RES_i \quad (12)$$

Additionally, we consider the Equal Error Rate (EER), a widely used metric in the literature. The EER corresponds to the error rate at the operational threshold τ where $BPCER(\tau) = APCER(\tau)$, providing a single-value summary of system performance.

⁸<https://www.iso.org/standard/79520.html>

6. Experimental Results

This section evaluates the performance of our proposed FakeIDet2. The performance results included in all tables are at ID level, not patch level, over the final evaluation datasets. This facilitates the comparison of our proposed FakeIDet2 with traditional approaches in the literature, focused on the whole ID level evaluation.

First, we evaluate the technical novelties of our proposal. Sec. 6.1 provides a comprehensive comparison in terms of the softmax-based loss functions. The analysis of the optimal patch size configuration and anonymization level is carried out in Sec. 6.2 and Sec. 6.3, respectively. Finally, for completeness, we compare FakeIDet2 with our previous FakeIDet [23]. These first experiments are carried out using our novel FakeIDet2-db, as described in Sec. 5.2.

Once the preliminary analysis is conducted using our novel FakeIDet2-db, we select the optimal configuration balancing performance and privacy and use it to evaluate FakeIDet2 in two common scenarios for PAD. The first scenario is introduced in Sec. 6.4, which studies the performance of FakeIDet2 to unseen attacks. Hence, we train FakeIDet2 with the optimal configuration leaving one of the PAIs out of the training set. The second scenario, Sec. 6.5, analyzes the performance of FakeIDet2 when it is exposed to images taken with smartphones cameras which has not seen in training. To do so, we train FakeIDet2 using images from all camera sensors except one. Finally, we evaluate in Sec. 6.6 the best configuration of FakeIDet2 in a cross-database scenario, providing a standard public benchmark to the research community.

6.1. Selecting the Optimal Loss Function Configuration

Given that different softmax-based loss functions are considered in FakeIDet2 training, we perform a comparison in terms of performance using the 128×128 , Non-Anonymized configuration. For each loss function, we also compare our proposed dynamic class weights (Dynamic-Weights) described in Sec. 4.1 with traditional approaches considered in the literature:

- *No-Weights*: All classes have a fixed weight equal to one.
- *Static-Weights*: Each class has its own weight based on their frequency in the dataset (Eq. 5), and it is kept fixed along the training.

Table 4 shows the results for the different loss functions, considering our proposed dynamic class weights. We observe that for all loss functions, Dynamic-Weights achieves better overall results. For example, in the case of CosFace we see that the No-Weights and Static-Weights configurations achieve practically the same results with 4.32% EER, while the Dynamic-Weights improves a bit the performance, with 3.66% EER. ArcFace shows minor improvements using Dynamic-Weights, with an improvement of 0.34% EER and 1.67% EER with respect to using Static-Weights and No-Weights, respectively. The best performance is obtained with AdaFace using Dynamic-Weights, with 2.01% EER, providing an improvement of 1.65% EER over No-Weights, and 4.30% EER over Static-Weights.

Additionally, in order to prove that the improvement in performance correlates with how the embedded space is modeled, we plot in Fig. 7 the embeddings distributions of AdaFace using t-SNE projection into 2D. In the figure, we show

Model	Screen	Print	Composite	All
<i>CosFace</i> [38]				
No-Weights	3.00	1.00	6.12	4.32
Static-Weights	1.02	3.89	7.17	4.32
Dynamic-Weights	4.00	0.00	4.08	3.66
<i>ArcFace</i> [10]				
No-Weights	6.00	6.77	10.21	7.32
Static-Weights	5.08	5.83	8.17	5.99
Dynamic-Weights	1.12	2.89	7.13	5.65
<i>AdaFace</i> [17]				
No-Weights	6.23	0.00	4.08	3.66
Static-Weights	6.00	7.77	5.12	6.31
Dynamic-Weights	1.23	0.12	2.09	2.01

Table 4: Results in terms of EER (%) for the different loss functions (CosFace, ArcFace and AdaFace) through our proposed dynamic class weights (Dynamic-Weights). Dynamic-Weights allows to deal with class imbalance among the different PAIs patches. Results are achieved using the final evaluation of FakeIDet2-db, considering the configuration 128×128 Non-Anonymized.

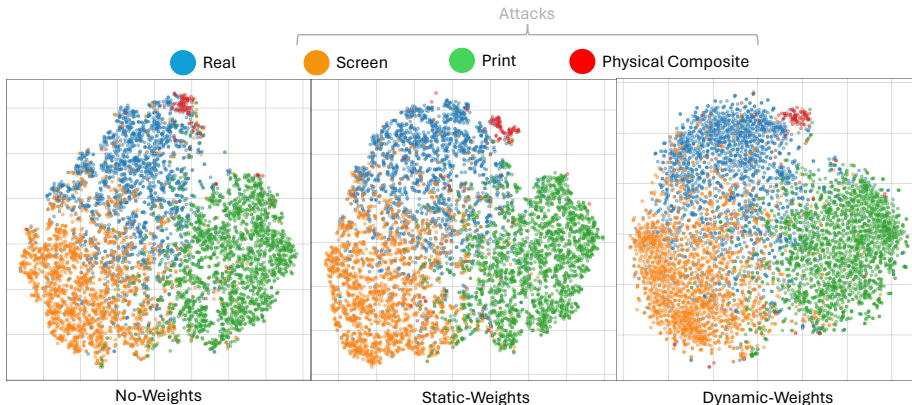


Figure 7: Differences of AdaFace’s learned embedding space using No-Weights (left), Static-Weights (middle), and Dynamic-Weights (right) via t-SNE 2D.

visual examples when: *i*) No-Weights are applied (left), *ii*) Static-Weights are applied (middle), and *iii*) Dynamic-Weights are applied (right). The data used for this visualization was randomly sampled from the test set, comprising 6,000 patches.

In the No-Weights case, we observe that physical composite patches (red points) overlap with real patches (blue points). This is a critical issue, as confusion between these two classes can significantly hinder the detection of physical composite attacks at the document level—indicating that the embeddings are not sufficiently discriminative.

For Static-Weights, we observe a clearer clustering trend for physical composite patches. However, as expected, keeping the weight values fixed throughout

Model	Screen	Print	Composite	All
<i>Whole ID</i>				
DINOv2[26]	21.85	11.35	24.68	22.63
<i>Patch Size: 128×128</i>				
FakeIDet [23]	7.10	0.00	54.08	25.58
FakeIDet2	1.23	0.12	2.09	2.01
<i>Patch Size: 64×64</i>				
FakeIDet [23]	9.00	0.00	58.17	26.25
FakeIDet2	4.53	1.45	7.17	3.99

Table 5: Performance results for the fine-tuned DINOv2 (whole ID), FakeIDet [23], and proposed FakeIDet2 in terms of EER. Results are achieved using the evaluation set of FakeIDet2-db. The Non-Anonymized configuration is selected to simulate current scenarios in literature.

training biases the model away from properly clustering patches from the other classes (i.e., real, print, and screen), which appear more scattered across the embedding space.

In contrast, with our proposed Dynamic-Weights, we observe a clear separation between physical composite patches and those from the remaining classes. This is enabled by the initial class weights computed at the start of training. Moreover, the clustering of the other classes is more consistent, with less sparsity in the outer sections of the space and more sparsity in the center compared to No-Weights and Static-Weights, which indicates a more robust feature extraction. We attribute this to the later training stages, during which the adaptive weights guide the model to better cluster patches from the more prevalent classes in the dataset.

The results of this section showcase that our proposed dynamic class weights approach suits better the problematic scenario of heavy class-imbalance. In summary, we adopt AdaFace loss function with Dynamic-Weights for the rest of our experiments.

6.2. Patch Size vs. Performance

For this section, we consider the Non-Anonymized configuration in order to provide a direct comparison of our proposed FakeIDet2 approach, based on patches, with the current scenario in the literature, based on the whole Non-Anonymized ID. For completeness, we also include in the comparison our previous FakeIDet detector [23], trained using 128×128 and 64×64 patch sizes, similar to FakeIDet2. For the scenario of feeding the fake detector with the whole ID, we fine-tune DINOv2 [26] foundation model using a final sigmoid layer attached DINOv2’s output embedding.

Table 5 shows a comparison between the performance of the fine-tuned DINOv2 (whole ID), FakeIDet [23], and FakeIDet2 in terms of EER. Overall, we see that training on the whole ID does not achieve good results (22.63%), in contrast to our proposed patch-wise approach.

In the 128×128 configuration, we observe that FakeIDet2 performs better than FakeIDet at detecting fake IDs of type screen (1.23% vs. 7.10% EER) and composite (2.09% vs. 54.08% EER), and remains close to FakeIDet in detecting

Model	Screen	Print	Composite	All
<i>Non-Anonymized</i>	4.53	1.45	7.17	3.99
<i>Pseudo-Anonymized</i>	5.01	4.89	16.29	8.64
<i>Fully-Anonymized</i>	8.98	5.77	26.54	17.94

Table 6: Performance of FakeIDet2 in terms of EER (%) when training over the different anonymization levels for the 64×64 patch size configuration. Results are achieved using the final evaluation of FakeIDet2-db, considering Non-Anonymized IDs.

print fake IDs (0.12% vs. 0.00% EER). Additionally, we observe that for the physical composite fake IDs, FakeIDet performance drops to 54.08% EER, while FakeIDet2 accurately detects these types of fake IDs leveraging the patch feature extraction and fusion, achieving a 2.09% EER. The drop in terms of performance is attributed to how FakeIDet computes the document level score. Given all the patches from a real or fake ID, it computes a score per individual patch and fuse them all together using a simple average, that yields a final score at document level. FakeIDet is reliable if the considered PAIs have the same patterns in the whole image. For example, in the case of a screen or print fake ID, it has the same properties over the whole ID (i.e., traces or fingerprints from the fake ID), but this is not true for physical composite fake IDs, as the ID is mostly real with the exception of the altered sections, failing to detect these kind of fake IDs properly. Finally, in the 64×64 configuration, we can observe a similar trend, although performance seems to drop a bit in both FakeIDet and FakeIDet2.

These results prove the technical contributions of FakeIDet2 over FakeIDet [23], i.e., Patch Embedding Extractor and the Patch Embedding Fusion, that not only allows to detect attacks where the whole ID is a fake (i.e., print or screen), but also attacks where small sections are fake (i.e., composite). Given that the performance using the 64×64 patch size configuration is close to the 128×128 patch size, we select this patch size for further experiments, as it increases privacy in real-world settings, which is the main purpose of the study.

6.3. Anonymization vs. Performance

In this section we analyze the impact in performance when removing sensitive information from an ID. To do so, we train FakeIDet2 in the 64×64 patch size configuration at all anonymization levels, and evaluate the performance using Non-Anonymized data. This scenario simulates realistic real-world settings in which ID Holders have some restrictions when sharing IDs to AI Researchers in order to train the fake ID detectors. Table 6 shows the performance of FakeIDet2 in terms of EER (%) for the different anonymization levels and attacks. A particular trend can be observed, as performance per attack and overall shows that the EER increases as the amount of sensitive information decreases, which shows that FakeIDet2 performance depends on the amount of sensitive information available in the training stage (3.99% in Non-Anonymized vs. 8.64% in Pseudo-Anonymized vs. 17.94% in Fully-Anonymized). Even with this drop in terms of performance, we observe that the Pseudo-Anonymized 64×64 configuration performs fairly well for only having seen partial information of the ID, which support our proposed hypothesis that training a model not using all the sensitive information of the ID produces quite competitive results and a small loss in performance as a trade-off. Given that this preliminary analysis

Training	Screen	Print	Composite	All
No-Screen	36.00	1.00	7.17	19.93
No-Print	3.05	6.77	12.25	7.97
No-Composite	2.02	0.00	50.96	28.24
All-Attacks	5.01	4.89	16.29	8.64

Table 7: Performance of FakeIDet2 in terms of EER (%) for the leave-one-attack-out scenario, i.e., leaving one of the PAIs out from the training dataset. These results are obtained evaluating with all PAIs, including the one left out in each case.

confirmed that training with Pseudo-Anonymized data using 64×64 patch size remains competitive, we decided to use this configuration for the rest of our experiments as it is balanced in terms of privacy and performance, which is the purpose of the study.

6.4. Leave-One-Attack-Out Scenario

Table 7 provides the results of FakeIDet2 when leaving different attacks out of the training data. For completeness, we include the EER for FakeIDet2 when trained using all PAIs available (All-Attacks). Based on our previous findings, we consider for training FakeIDet2 the Pseudo-Anonymized 64×64 patch configuration, due to privacy reasons. The final evaluation is carried using Non-Anonymized 64×64 patch configuration.

The worst results in terms of EER are obtained when composite attacks are left out, with a 28.24% when evaluating across all types of attacks. This shows that the physical composite attacks included in our novel FakeIDet2-db are the harder attacks for our model to detect, with 50.96% EER. It is also interesting to highlight that our screen attacks seem difficult to detect when they are out of training, with 36.00% EER. Finally, in the case of the print attacks, FakeIDet2 performs much better compared to detecting the other attacks with just a 6.77% in terms of EER when only detecting print attacks, although a little caveat should be considered. As covered in Sec. 3, our physical composite attacks are created by using small crops from print attacks, and lying them over real IDs. We argue that FakeIDet2 may be leveraging those learned features from composite patches to predict print attacks appropriately, giving competitive results that even improve the performance when the whole dataset is available (8.64% EER vs. 7.97% EER).

Finally, an interesting phenomena is observed when training FakeIDet2 leaving one attack out: the fake detector seems to “specialize” in detecting the attacks that are used in training, since the EER becomes even lower compared to the case of training using all attacks. For example, when leaving the composite attacks, FakeIDet2 obtains an EER of 2.02% when detecting print attacks, compared to 5.01% which is obtained when trained with all attacks. This can be expected, as when the number of classes is smaller, the data distribution to model by FakeIDet2 becomes simpler, hence becoming better at detecting the only attacks presented at training time.

6.5. Leave-One-Sensor-Out Scenario

Table 8 provides the results of FakeIDet2 when leaving different acquisition sensors out of the training data. For completeness, we include the EER for

Model	Screen	Print	Composite	All
No-iPhone	22.12	30.98	30.63	22.61
No-Xiaomi	3.96	1.94	14.24	8.30
No-Redmi	8.07	1.94	7.13	8.97
All-Devices	5.01	4.89	16.29	8.64

Table 8: Performance of FakeIDet2 in terms of EER (%) for the leave-one-sensor-out scenario, i.e., leaving one of the acquisition devices out from the training dataset. These results are obtained evaluating with data from all the acquisition devices in the Non-Anonymized, 64×64 patch configuration including the one left out in each case.

FakeIDet2 when trained using all devices available (All-Devices). Based on our previous findings, we consider for training FakeIDet2 the Pseudo-Anonymized 64×64 patch configuration, due to privacy reasons. The final evaluation is carried using Non-Anonymized 64×64 patch configuration.

As can be seen in the table, performance drops when the sensor with the highest quality (i.e., iPhone 15) is not used in training but only in the final evaluation. This seems not to be happening in the rest of scenarios, where images from the iPhone 15 are present in the training set. Given the different experiments that we run regarding this issue, our intuition on why this is happening relies on the fact that iPhone 15 cameras capture finer details that give more distinct features compared to Xiaomi’s and Redmi’s sensors. These fine grain characteristics allow for our FakeIDet2 to focus on traces that are more subtle, such as Moiré patterns on the screen attacks and the droplets of ink from the print and composite attacks, given that these attacks were printed with a Inkjet-kind printer. Furthermore, one of the main features of AdaFace loss function is that the adaptive margins change depending on the image quality. When using images of high-quality along with low- or medium-quality, the database is more diverse, and AdaFace helps the learning process by establishing larger margins to high-quality images and lower to low-quality. If images of low-quality are the majority of the database, the margins may not be as large as desired for proper separation between classes, and the features per each class may be overlapped in the embedded space, which are not helpful when forwarded into the Patch Embedding Fusion module, harming the performance. Evidences of this is the fact that results when images from the iPhone 15 camera are present, the evaluation performance of FakeIDet2 seems to be similar in both cases (i.e., No-Xiaomi vs. No-Redmi vs. All-Devices).

6.6. Cross-Database Scenario

This section evaluates the performance of FakeIDet2 trained through the selected configuration (i.e., Pseudo-Anonymized 64×64 patch size) on different public databases in the literature. Concretely, we consider DLC-2021 [30], KID34K [27] and Benalcazar *et al.* synthetic database from [5]. For this evaluation, we sample around 10,000 images from KID34K, balancing across PAIs and ID owners, and roughly 30,000 images from several videos of DLC-2021, sampling in a similar way as in KID34K. DLC-2021 contains Spanish IDs, but they are from the first version, which are not seen during training FakeIDet2 as described in Sec. 5.1. Regarding the real IDs, as in those databases the “real” IDs were created by the researchers in laboratory conditions, i.e., they

PAI	DLC-2021 [30]	KID34K [27]	Benalcazar <i>et al.</i> [5]
Screen	5.02	13.41	N/A
HQ-Print	10.28	18.26	N/A
Print	12.45	4.99	N/A
Gray-Print	10.60	N/A	N/A
Synthetic	N/A	N/A	39.41
All	8.90	13.84	39.41

Table 9: Performance of FakeIDet2 in terms of EER (%) per type of attack and database. In order to facilitate the collaboration between ID Holders and AI Researchers, we consider the privacy-aware scenario where FakeIDet2 is trained using the Pseudo-Anonymized 64×64 patch size configuration.

are not official IDs, we consider the aforementioned databases as attacks. Real IDs are extracted from the evaluation dataset of our FakeIDet2-db, similar to previous experiments, as they are official IDs. Our aim with this privacy-aware scenario is to assess the generalization ability of our proposed FakeIDet2 to unseen conditions, e.g., different PAIs, templates, devices, etc.

Table 9 shows the performance of FakeIDet2 in terms of EER (%) per type of attack and database. In order to facilitate the collaboration between ID Holders and AI Researchers, we consider the privacy-aware scenario where FakeIDet2 is trained using the Pseudo-Anonymized 64×64 patch size configuration. For DLC-2021 and KID34K we denote as “HQ-print” the types of print attacks which are proposed as “real” in each of the databases, and for Benalcazar *et al.* we denote “Synthetic” for the samples that have been created via generative methods trained from real samples. Additionally, in case a database does not contain a specific attack, it is denoted as “N/A”.

As can be seen in Table 9, the performance per PAI varies among databases. For instance, FakeIDet2 seems to perform worst in screen attacks from the KID34K database compared to the DLC-2021, with 13.41% vs. 5.02%, respectively. This could be motivated by the amount of devices which were used for screen attack creation in KID34K, which varied from smartphones, tablets, laptops, and LCD monitors. A similar trend can be observed for the HQ-print attacks, where KID34K samples seem to confuse FakeIDet2 more (18.26% vs. 10.28%). This may be induced due to the variability in terms of acquisition devices (12 in KID34K vs. 2 in DLC-2021), with different specifications that create different traces or fingerprints in the images taken. Regarding print attacks, we see that our model performs better on the KID34K dataset than in DLC-2021 (4.99% vs. 12.45%). This might be produced as KID34K follows a similar approach to ours, i.e., print attacks are created after printed and then laminated. Finally, for the synthetic attacks included in Benalcazar *et al.* database, FakeIDet2 is not able to generalize well to this unseen attack (39.41% EER). This result is expected due to the following reasons: *i*) the data (both real and fake ID samples) used to train FakeIDet2 is only based on physical acquisitions using smartphone cameras, not synthetic data, and *ii*) according to [5], those synthetic samples were generated using GANs trained with official Chilean ID samples, which means they share similar characteristics with real IDs that may be confusing FakeIDet2.

In conclusion, our proposed privacy-aware scenario in order to promote the collaboration between ID Holders and AI Researchers has provided very interesting results, despite of the fact that our proposed FakeIDet2 is only trained through the Pseudo-Anonymized 64×64 patch size configuration, using the the development set of FakeIDet2-db. Under unseen physical attacks, FakeIDet2 is able to achieve 8.90% EER on DLC-2021 and 13.84% on KID34K, as can be seen in Table 9. We expect these results will further improve in real-world settings, as the ID Holders own large-scale ID databases.

7. Conclusion

In this article we have explored a novel framework for privacy-aware fake ID detection, which bridges the existing gap between IDs Holders (e.g., governments, police, banks, etc.), which provide digital services to citizens and own large-scale datasets of real IDs, and the AI Researchers, which have the experience and technology to develop fake ID detectors, but not the data.

In order to advance in the field, we have first introduced FakeIDet2-db, a database that complies with the proposed framework, which contains over 900K patches in different sizes (128×128 and 64×64), extracted from a total of 2,000 images of pseudo- and fully-anonymized IDs. Regarding real and fake IDs, to the best of our knowledge this is the first database that contains: *i*) official real IDs captured under several conditions regarding camera sensor, illumination conditions and distance, and *ii*) physical composite attacks. In addition, our database considers a large variability during the acquisition, e.g., using three different smartphones, and changes in illumination and height conditions.

Along with FakeIDet2-db, we have presented FakeIDet2, a new method for privacy-aware fake ID detection that leverages patches from IDs and varying levels of anonymization to safeguard the sensitive information. We demonstrate that learning embeddings from patches extracted from real and fake IDs is a crucial step for effective fake ID detection. Considering the nature of the problem, especially for physical composite attacks, we have proposed a method that explicitly accounts for class imbalance, achieving superior performance compared to traditional approaches. Using patch-level embeddings, we have incorporated a learnable fusion module based on MHSA to model the relationships between patches within a single ID, producing a ID-level prediction indicating whether the submitted ID is real or fake. Additionally, we have evaluated the impact of different anonymization levels and patch sizes, showing that our FakeIDet2 remains competitive in privacy-aware scenarios, as compared to fully visible data settings (3.99% in non-anonymized vs. 8.64% in pseudo-anonymized).

Finally, we have also introduced an extensive and reproducible public benchmark, which considers in addition to our FakeIDet2-db, other public databases in the literature, containing unseen physical (KID34K [27], DLC-2021 [30]) and synthetic attacks (Benalcazar *et al.* [5]) to assess the performance on different data distributions that contain IDs from several demographic regions (i.e., Europe, Asia and South America).

The results achieved by FakeIDet2 (Pseudo-Anonymized 64×64 patch size configuration) in the proposed benchmark under unseen conditions, 8.90% EER on DLC-2021 and 13.84% on KID34K, promote our proposed privacy-aware scenario in order to facilitate the collaboration between ID Holders and AI Researchers in real-world settings.

Acknowledgements

Funding from INTER-ACTION (PID2021-126521OBI00 MICINN/FEDER), M2RAI (PID2024-160053OB-I00 MICIU/FEDER), Cátedra ENIA UAM-Veridas en IA Responsable (NextGenerationEU PRTR TSI-100927-2023-2), and PowerAI+ (SI4/PJI/2024-00062 Comunidad de Madrid and UAM).

References

- [1] Arlazarov, V.V., Bulatov, K., Chernov, T., Arlazarov, V.L., 2019. MIDV-500: A Dataset for Identity Document Analysis and Recognition on Mobile Devices in Video Stream. *Computer Optics* 43.
- [2] Aslett, K., Sanderson, Z., Godel, W., Persily, N., Nagler, J., Tucker, J.A., 2024. Online Searches to Evaluate Misinformation Can Increase Its Perceived Veracity. *Nature* 625, 548–556.
- [3] Ba, J.L., Kiros, J.R., Hinton, G.E., 2016. Layer Normalization. *arXiv preprint arXiv:1607.06450* URL: <https://arxiv.org/abs/1607.06450>, *arXiv:1607.06450*.
- [4] Bahdanau, D., Cho, K., Bengio, Y., 2016. Neural Machine Translation by Jointly Learning to Align and Translate. URL: <https://arxiv.org/abs/1409.0473>, *arXiv:1409.0473*.
- [5] Benalcazar, D., Tapia, J.E., Gonzalez, S., Busch, C., 2023. Synthetic ID Card Image Generation for Improving Presentation Attack Detection. *IEEE Transactions on Information Forensics and Security* 18, 1814–1824.
- [6] Bengio, Y., Courville, A., Vincent, P., 2013. Representation Learning: A Review and New Perspectives. *IEEE Transactions on Pattern Analysis and Machine Intelligence* 35, 1798–1828.
- [7] Bulatov, K., Emelianova, E., Tropin, D., et al., 2022. MIDV-2020: A Comprehensive Benchmark Dataset for Identity Document Analysis. *Computer Optics* 46.
- [8] Bulatov, K., Matalov, D., Arlazarov, V.V., 2020. MIDV-2019: Challenges of the Modern Mobile-Based Document OCR, in: *Proceedings of the International Conference on Machine Vision*, pp. 818–824.
- [9] Chen, T., Kornblith, S., Norouzi, M., Hinton, G., 2020. A Simple Framework for Contrastive Learning of Visual Representations, in: *Proceedings of the International Conference on Machine Learning*, pp. 1597–1607.
- [10] Deng, J., Guo, J., Xue, N., Zafeiriou, S., 2019. ArcFace: Additive Angular Margin Loss for Deep Face Recognition, in: *Proceedings of the IEEE/CVF Conference on Computer Vision and Pattern Recognition*, pp. 4690–4699.
- [11] Fang, M., Huber, M., Fierrez, J., et al., 2023. SynFacePAD 2023: Competition on Face Presentation Attack Detection Based on Privacy-aware Synthetic Training Data, in: *IEEE/IAPR International Joint Conference on Biometrics*, pp. 1–11.

- [12] Feng, S., Tramèr, F., 2024. Privacy Backdoors: Stealing Data with Corrupted Pretrained Models, in: Proceedings of the 41st International Conference on Machine Learning, pp. 13326–13364.
- [13] Gonzalez, S., Tapia, J.E., 2025. Forged Presentation Attack Detection for ID Cards on Remote Verification Systems. *Pattern Recognition* 162, 111352.
- [14] He, K., Zhang, X., Ren, S., Sun, J., 2016. Deep Residual Learning for Image Recognition, in: Proceedings of the IEEE/CVF Conference on Computer Vision and Pattern Recognition, pp. 770–778.
- [15] Hernandez-Ortega, J., Fierrez, J., Morales, A., Galbally, J., 2023. Introduction to Presentation Attack Detection in Face Biometrics and Recent Advances, in: S. Marcel, J. Fierrez, N.E. (Ed.), *Handbook of Biometric Anti-Spoofing*, Springer. pp. 203–230. doi:https://doi.org/10.1007/978-981-19-5288-3_9. 3rd Ed.
- [16] Jaipuria, N., Zhang, X., Bhasin, R., Arafa, M., Chakravarty, P., Shrivastava, S., Manglani, S., Murali, V.N., 2020. Deflating Dataset Bias Using Synthetic Data Augmentation, in: Proceedings IEEE/CVF Conference on Computer Vision and Pattern Recognition Workshops, pp. 772–773.
- [17] Kim, M., Jain, A.K., Liu, X., 2022. Adaface: Quality Adaptive Margin for Face Recognition, in: Proceedings of the IEEE/CVF Conference on Computer Vision and Pattern Recognition, pp. 18750–18759.
- [18] Liu, H., Wang, W., Sun, H., Rocha, A., Li, H., 2024. Robust Domain Misinformation Detection via Multi-Modal Feature Alignment. *IEEE Transactions on Information Forensics and Security* 19, 793–806.
- [19] Markham, R.P., López, J.M.E., Nieto-Hidalgo, M., Tapia, J.E., 2024. Open-Set: ID Card Presentation Attack Detection Using Neural Style Transfer. *IEEE Access* 12, 68573–68585.
- [20] Melzi, P., Rathgeb, C., Tolosana, R., Vera-Rodriguez, R., Lawatsch, D., Domin, F., Schaubert, M., 2023. GANDiffFace: Controllable Generation of Synthetic Datasets for Face Recognition with Realistic Variations, in: Proceedings of the IEEE/CVF International Conference on Computer Vision Workshops, pp. 3086–3095.
- [21] Melzi, P., Tolosana, R., Vera-Rodriguez, R., Kim, M., Rathgeb, C., Liu, X., DeAndres-Tame, I., Morales, A., Fierrez, J., Ortega-Garcia, J., et al., 2024. FRCSyn-onGoing: Benchmarking and Comprehensive Evaluation of Real and Synthetic Data to Improve Face Recognition Systems. *Information Fusion* 107, 102322.
- [22] Mudgalgundurao, R., Schuch, P., Raja, K., Ramachandra, R., Damer, N., 2022. Pixel-Wise Supervision for Presentation Attack Detection on Identity Document Cards. *IET Biometrics* URL: <https://doi.org/10.1049/bme2.12088>.

- [23] Muñoz-Haro, J., Tolosana, R., Vera-Rodriguez, R., Morales, A., Fierrez, J., 2025. FakeIDet: Exploring Patches for Privacy-Preserving Fake ID Detection, in: Proceedings IEEE/IAPR International Joint Conference on Biometrics. URL: <https://arxiv.org/abs/2504.07761>.
- [24] Ooi, K.B., Tan, G.W.H., Al-Emran, M., Al-Sharafi, M.A., Capatina, A., Chakraborty, A., Dwivedi, Y.K., Huang, T.L., Kar, A.K., Lee, V.H., Loh, X.M., Micu, A., Mikalef, P., Mogaji, E., Pandey, N., Raman, R., Rana, N.P., Sarker, P., Sharma, A., Teng, C.I., Wamba, S.F., and, L.W.W., 2025. The Potential of Generative Artificial Intelligence Across Disciplines: Perspectives and Future Directions. *Journal of Computer Information Systems* 65, 76–107.
- [25] van den Oord, A., Li, Y., Vinyals, O., 2019. Representation Learning with Contrastive Predictive Coding. URL: <https://arxiv.org/abs/1807.03748>, arXiv:1807.03748.
- [26] Oquab, M., Darcet, T., Moutakanni, T., Vo, H.V., Szafraniec, M., Khaidov, V., Fernandez, P., HAZIZA, D., Massa, F., El-Nouby, A., Assran, M., Ballas, N., Galuba, W., Howes, R., Huang, P.Y., Li, S.W., Misra, I., Rabbat, M., Sharma, V., Synnaeve, G., Xu, H., Jegou, H., Mairal, J., Labatut, P., Joulin, A., Bojanowski, P., 2024. DINOv2: Learning Robust Visual Features Without Supervision. *Transactions on Machine Learning Research*.
- [27] Park, E.J., Back, S.Y., Kim, J., Woo, S.S., 2023. KID34K: A Dataset for Online Identity Card Fraud Detection, in: Proceedings of the 32nd ACM International Conference on Information and Knowledge Management, Association for Computing Machinery. pp. 5381–5385.
- [28] Pernuš, M., Fookes, C., Štruc, V., Dobrišek, S., 2025. FICE: Text-Conditioned Fashion-Image Editing with Guided GAN Inversion. *Pattern Recognition* 158, 111022.
- [29] Peña, A., Fierrez, J., Morales, A., Mancera, G., Lopez, M., Tolosana, R., 2025. Addressing Bias in LLMs: Strategies and Application to Fair AI-based Recruitment, in: Proceedings AAAI/ACM Conference on AI, Ethics, and Society. URL: <https://arxiv.org/abs/2506.11880>.
- [30] Poleyov, D.V., Sigareva, I.V., Ershova, D.M., et al., 2022. Document Liveness Challenge Dataset (DLC-2021). *Journal of Imaging* 8.
- [31] Shahreza, H.O., Ecabert, C., George, A., Unnervik, A., Marcel, S., Di Domenico, N., Borghi, G., Maltoni, D., Boutros, F., Vogel, J., Damer, N., Sanchez-Perez, A., Mas-Candela, E., Calvo-Zaragoza, J., Biesseck, B., Vidal, P., Granada, R., Menotti, D., DeAndres-Tame, I., La Cava, S.M., Concas, S., Melzi, P., Tolosana, R., Vera-Rodriguez, R., Perelli, G., Orrù, G., Marcialis, G.L., Fierrez, J., 2024. SDFR: Synthetic Data for Face Recognition Competition, in: Proceedings 18th International Conference on Automatic Face and Gesture Recognition, pp. 1–9.
- [32] Soares, A., Batista, R., Leite, B., 2020. BID Dataset: a Challenge Dataset for Document Processing Tasks, in: Anais Estendidos da Conference on Graphics, Patterns and Images, pp. 143–146.

- [33] Tapia, J.E., Damer, N., Busch, C., et al., 2024. First Competition on Presentation Attack Detection on ID Card, in: Proceedings of the IEEE International Joint Conference on Biometrics, pp. 1–10.
- [34] Tolosana, R., Vera-Rodriguez, R., Fierrez, J., Morales, A., Ortega-Garcia, J., 2020. Deepfakes and Beyond: A Survey of Face Manipulation and Fake Detection. *Information Fusion* 64, 131–148.
- [35] Tolosana, R., Vera-Rodriguez, R., Fierrez, J., Morales, A., Ortega-Garcia, J., 2022. An introduction to digital face manipulation, in: Rathgeb, C., et al. (Eds.), *Handbook of Digital Face Manipulation and Detection*, Springer. pp. 3–26.
- [36] Vaswani, A., Shazeer, N., Parmar, N., et al., 2017. Attention Is All You Need, in: *Proceedings Advances in Neural Information Processing Systems*, pp. 6000–6010.
- [37] Verdoliva, L., 2020. Media Forensics and DeepFakes: An Overview. *IEEE Journal of Selected Topics in Signal Processing* 14, 910–932.
- [38] Wang, H., Wang, Y., Zhou, Z., Ji, X., Gong, D., Zhou, J., Li, Z., Liu, W., 2018. Cosface: Large margin cosine loss for deep face recognition, in: *Proceedings of the IEEE/CVF Conference on Computer Vision and Pattern Recognition*, pp. 5265–5274.
- [39] Xie, L., Wang, Y., Guan, H., Nag, S., Goel, R., Swamy, N., Yang, Y., Xiao, C., Prisby, J., Maciejewski, R., Zou, J., 2024. IDNet: A Novel Identity Document Dataset via Few-Shot and Quality-Driven Synthetic Data Generation, in: *Proceedings of the IEEE International Conference on Big Data*, pp. 2244–2253.
- [40] Zhang, Y., Jia, R., Pei, H., Wang, W., Li, B., Song, D., 2020. The Secret Revealer: Generative Model-Inversion Attacks Against Deep Neural Networks, in: *Proceedings of the IEEE/CVF Conference on Computer Vision and Pattern Recognition*, pp. 250–258.